

Engineering Conferences International ECI Digital Archives

Electric Field Enhanced Processing of Advanced
Materials II: Complexities and Opportunities

Proceedings

3-10-2019

β -SiAlON-based ceramic composites by combustion synthesis and spark plasma sintering

Evgeny Grigoryev

ISMAN, Russia, eugengrig@mail.ru

Vladimir Goltsev

NRNU MEPhI

Konstantin Smirnov

ISMAN

Dmitriy Moskovskikh

NITU MISiS

Aleksey Sedegov

NITU MISiS

Follow this and additional works at: http://dc.engconfintl.org/efe_advancedmaterials_ii



Part of the [Materials Science and Engineering Commons](#)

Recommended Citation

Evgeny Grigoryev, Vladimir Goltsev, Konstantin Smirnov, Dmitriy Moskovskikh, and Aleksey Sedegov, " β -SiAlON-based ceramic composites by combustion synthesis and spark plasma sintering" in "Electric Field Enhanced Processing of Advanced Materials II: Complexities and Opportunities", Rishi Raj, University of Colorado, USA Olivier Guillon, Forschungszentrum Jülich, Germany Hidehiro Yoshida, National Institute for Materials Science, Japan Eds, ECI Symposium Series, (2019). http://dc.engconfintl.org/efe_advancedmaterials_ii/13

This Abstract and Presentation is brought to you for free and open access by the Proceedings at ECI Digital Archives. It has been accepted for inclusion in Electric Field Enhanced Processing of Advanced Materials II: Complexities and Opportunities by an authorized administrator of ECI Digital Archives. For more information, please contact franco@bepress.com.

β -SiAlON-Based Ceramic Composites by Combustion Synthesis and Spark Plasma Sintering

K.L. Smirnov¹, V.Y. Goltsev², E.G. Grigoryev¹, D.O. Moskovskikh³, A.S. Sedegov³

¹Merzhanov Institute of Structural Macrokinetics and Materials Science, Russian Academy of Sciences, Chernogolovka, Moscow region, Russia

²National Research Nuclear University MEPhI, Moscow, Russia, ³National University of Science and Technology MISiS, Moscow, Russia

Introduction

Solid solutions of general formula $Si_{6-z}Al_zO_zN_{8-z}$ ($z = 0.0-4.2$) are known for their excellent hardness, strength, and wear/corrosion resistance, which explains their wide use in various engineering applications such as refractory materials, bearings, and cutting instruments [1]. Functionality of β -SiAlON ceramics can be markedly improved upon addition of other refractory compounds with strongly different physical parameters such as Young modulus, thermal/electrical conductivity, thermal expansion, etc. The addition of hexagonal boron nitride (h-BN), TiN, and SiC to ceramic composites is known to improve their fracture toughness, thermal shock resistance, tribological properties, thermal/electrical conductivity, and machinability.

Combustion synthesis (CS) is a rapidly developing research area oriented on fast and energy efficient production of high-melting compounds and materials. For example, infiltration-mediated CS in nitrogen is a convenient technique for production of α - and β -SiAlON powders with different phase and elemental composition, particle size, and morphology [2]. Spark plasma sintering (SPS) is a newly developed process that uses dc pulses for sample heating. As compared to conventional hot pressing, SPS ensures higher heating rates and very short holding times and has been widely recognized as a rapid and effective method for densification of various materials [3]. So the combination of CS and SPS techniques seems rather promising for R & D of β -SiAlON-based ceramics with widened functionality.

Keywords - combustion synthesis; spark plasma sintering; ceramic composites; silalons; boron nitride; titanium nitride; silicon carbide

Experimental

Infiltration-mediated CS of β -Si₂AlON₇ and h-BN powders in nitrogen gas was carried out by the following schemes: Green mixtures also contained some amount of homemade diluents, β -Si₂AlON₇ and h-BN respectively, in order to improve extent of conversion. Combustion was performed in a 2-L reactor at $P(N_2) = 8-10$ MPa. The CS of β -SiC was carried out by using multistep chemical reactions in the Si-C-N system [4] and TiN fine powders with added NH₄Cl as a gasifying agent [5]. Aliquot amounts of combustion-synthesized raw powders were intermixed in a high-energy planetary steel-ball mill. Ball milling time (800 rpm, ball/mill ratio 10 : 1) was 5 min. Then milled powders (about 0.5 g) were placed into a graphite die 10.4 mm in inner diameter and sintered in a Labox 625 SPS facility under vacuum (below 10 Pa). The pieces of carbon paper and carbon felt were put between the powder and graphite die to exclude high-temperature reaction during sintering, as well as to easily get the sample out after sintering. The heating rate was 50 deg/min. The sintered compacts were heated from room temperature to 600°C without applied load and then to 1550–1800°C at a compressive stress of 50 MPa. The compacts were held at a desired temperature for 5 min before the power was turned off. Temperature monitoring during sintering between 600°C and final sintering temperature was carried out using an optical pyrometer focused on a hole in the carbon die. The particle size distribution of milled powders was determined with Fritsch Analysette 22 device. The BET analysis (N₂ sorption) was performed by using a Sorbi-M surface area analyzer. The raw powders and sintered compacts were characterized by XRD (DRON-3.0) and SEM (JEOL 6610L). Sample densities were determined by hydrostatic weighing. Flexural strength (σ_f) was measured for bending a thin disk on a ring base in a testing machine Instron-5966.

Results and Discussion

According to XRD results, the raw powders of β -Si₂AlON₇, h-BN, and TiN did not contain impurity phases while β -SiC had trace amounts of Si₃N₄. According to SEM results, all as-synthesized powders appeared largely as agglomerates (Fig. 1). Their specific surface was about 1.3 m²/g for β -Si₂AlON₇ powders, and from 9.8 to 22.8 m²/g for h-BN, β -SiC, and TiN fine powders. After ball milling, the specific surface increased by a factor of 4–6. Simultaneously, the particle size distribution of h-BN-containing mixtures always exhibited an additional peak around 20–60 μ m, thus indicating the formation of secondary huge agglomerates from initially fine particles.

Figures 2 and 3 show relative density ρ_{rel} of sintered samples as a function of temperature T . The sintering of pure β -Si₂AlON₇ was accompanied by marked intensification of the consolidation process at temperatures above 1400°C (curve 1 in Fig. 2) probably due to formation of SiO₂ and Al₂O₃ eutectics. Upon further increase in T , relative density of sintered β -Si₂AlON₇ gradually grows up to 87% (curve 1 in Fig. 3). Our SEM observations suggest (Fig. 4) that at 1550°C the particles remain practically unchanged (Fig. 4a) and the formation of bottle necks gets started at higher temperatures. According to XRD data, pure β -Si₂AlON₇ sintered above 1750°C exhibits the traces of AlN formed upon thermal decomposition of β -Si₂AlON₇. This is also evidenced by some increase in gas pressure in the SPS chamber observed above 1600°C caused by the release of appropriate gaseous decomposition products, N₂ and SiO. Note that the release of gaseous products was observed only for sintered materials with $\rho_{rel} < 87\%$. In case of denser materials with no open porosity, the decomposition of β -Si₂AlON₇ were completely suppressed. The addition of h-BN improves the compactibility of sintered powder mixtures. Under a compressive stress of 50 MPa at 600°C, the initial value of ρ_{rel} exceeds 80% for the compact containing 30 wt % BN and 60% for that of pure β -Si₂AlON₇ (Fig. 2).

In parallel, an increase in h-BN content suppresses the consolidation processes due to formation of liquid eutectics. At 30 wt % BN (curve 4 in Fig. 2), the temperature dependence of ρ_{rel} becomes much more aligned. As is seen in Fig. 5a (10 wt % BN), the small flaky h-BN particles are uniformly distributed over the surface of larger β -Si₂AlON₇ particulates. At 30 wt % BN (Fig. 5b), the h-BN particles (unwettable with oxide melt) fully separate the β -Si₂AlON₇ particles apart. It is clear that in such systems a contribution from liquid-phase processes to consolidation cannot be important. In case of 10 and 20 wt % h-BN, the processes associated with formation of liquid eutectics are more or less pronounced, so that high relative density (close to theoretical one) can be attained (see curve 3 in Fig. 3). The addition of fine β -SiC and TiN powders worsens the compactibility of sintered powder mixtures under a compressive stress at the initial stage (Fig. 6). As a result, the highest value of relative density for sintered ceramic composites containing β -SiC can only be achieved at 1750°C (curve 2 in Fig. 3). Meanwhile, the addition of TiN powder is seen to facilitate the efficiency of sintering above 900°C (curves 2, 3 in Fig. 6) and the highest values of ρ_{rel} can be achieved already at 1550°C (curve 4 in Fig. 3). Figure 7a illustrates flexural strength σ_f as a function of ρ_{rel} . Our results well agree with those reported for similar ceramic composites prepared by other techniques [6–7]. SPS method affords to produce ceramic composites with higher relative density and flexural strength (up to 400 MPa). In our case, the flexural strength of sintered ceramic composites was found to depend on the BN content only slightly (Fig. 8b). A marked increase in σ_f (up to 40%) can be achieved upon replacement of 40 wt % of relatively coarse β -SiAlON particles in sintered ceramic composites by finer β -SiC and TiN particles (curve 2 in Fig. 7a).

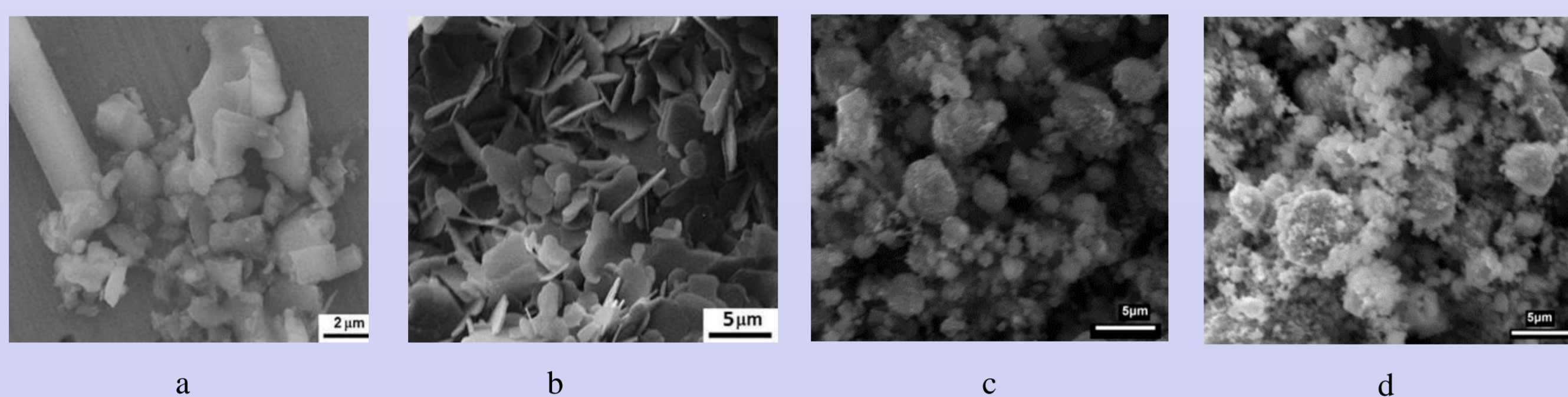


Figure 1. SEM images of starting β -Si₂AlON₇ (a), h-BN (b), β -SiC (c), and TiN (d) powders.

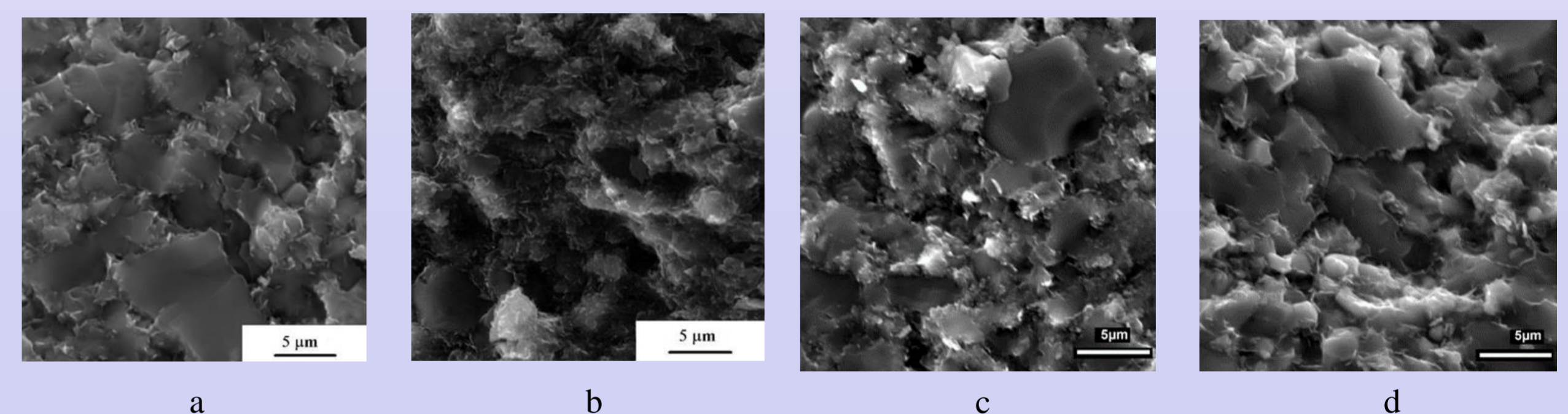


Figure 5. Fracture surface of sintered ceramic composites: (a) β -Si₂AlON₇-BN (10 wt %), (b) β -Si₂AlON₇-BN (30 wt %), (c) β -Si₂AlON₇-SiC (40 wt %)-BN (10 wt %), and (d) β -Si₂AlON₇-TiN (40 wt %)-BN (10 wt %); $T_{max} = 1750^\circ\text{C}$.

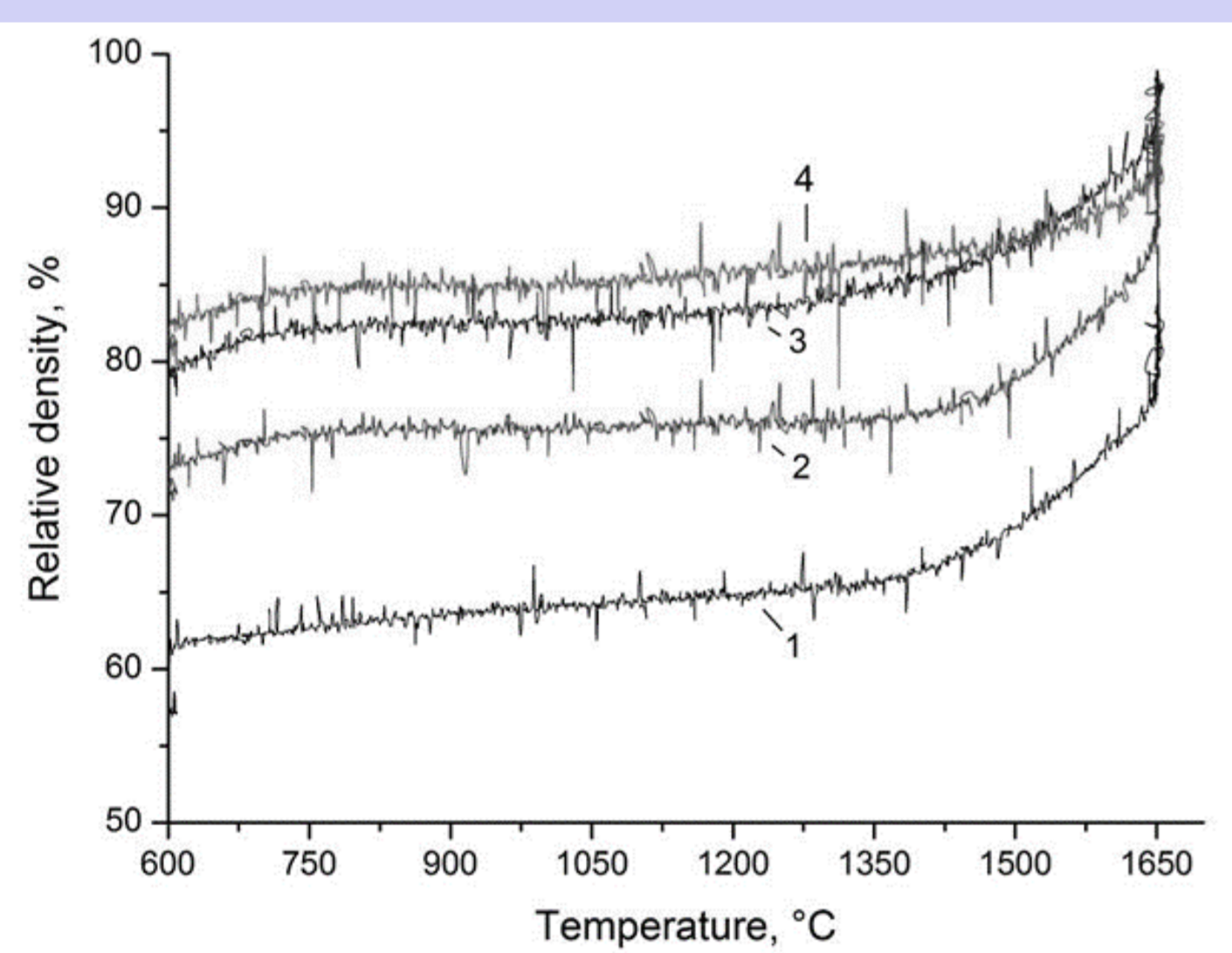


Figure 2. Relative density ρ_{rel} as a function of temperature T for: β -Si₂AlON₇ (1), β -Si₂AlON₇-BN (10 wt %) (2), β -Si₂AlON₇-BN (20 wt %) (3), and β -Si₂AlON₇-BN (30 wt %) (4); $T_{max} = 1650^\circ\text{C}$.

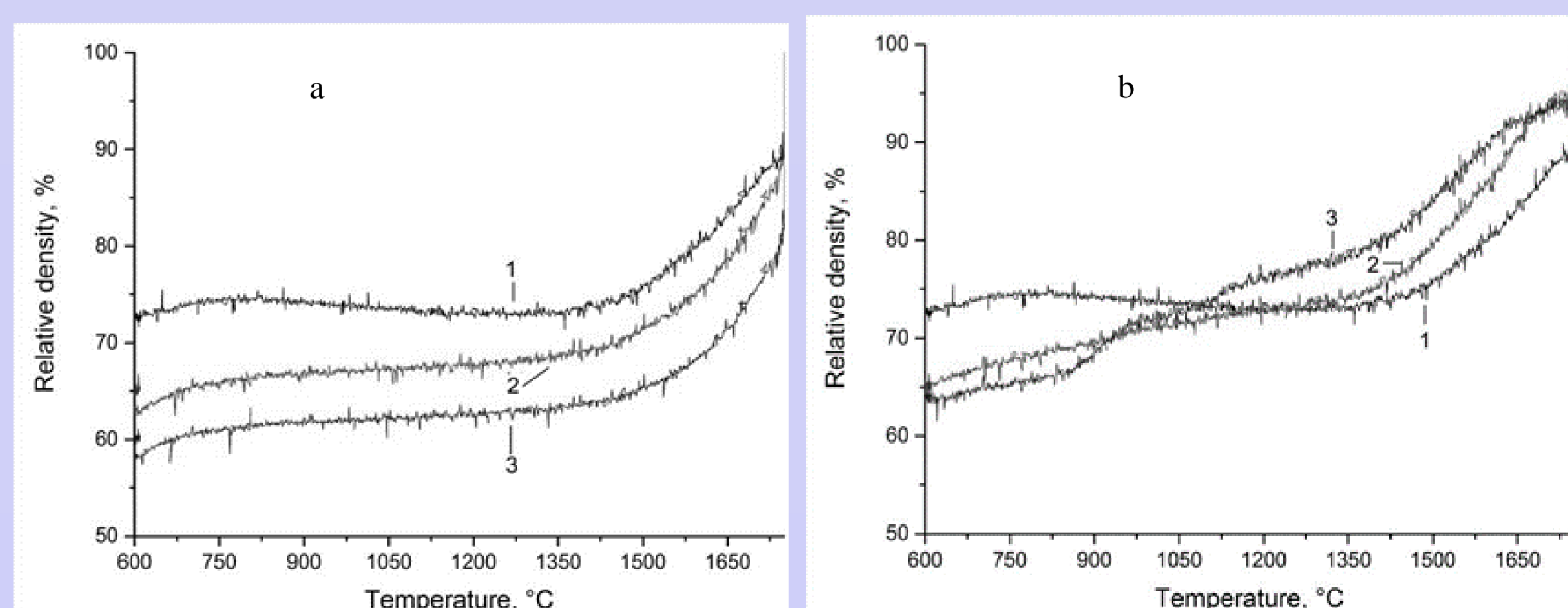


Figure 6. Relative density ρ_{rel} as a function of temperature T for: (a) β -Si₂AlON₇-BN (10 wt %) (1), β -Si₂AlON₇-SiC (20 wt %)-BN (10 wt %) (2), and β -Si₂AlON₇-SiC (40 wt %)-BN (10 wt %) (3); and (b) β -Si₂AlON₇-BN (10 wt %) (1), β -Si₂AlON₇-TiN (20 wt %)-BN (10 wt %) (2), and β -Si₂AlON₇-TiN (40 wt %)-BN (10 wt %) (3); $T_{max} = 1750^\circ\text{C}$.

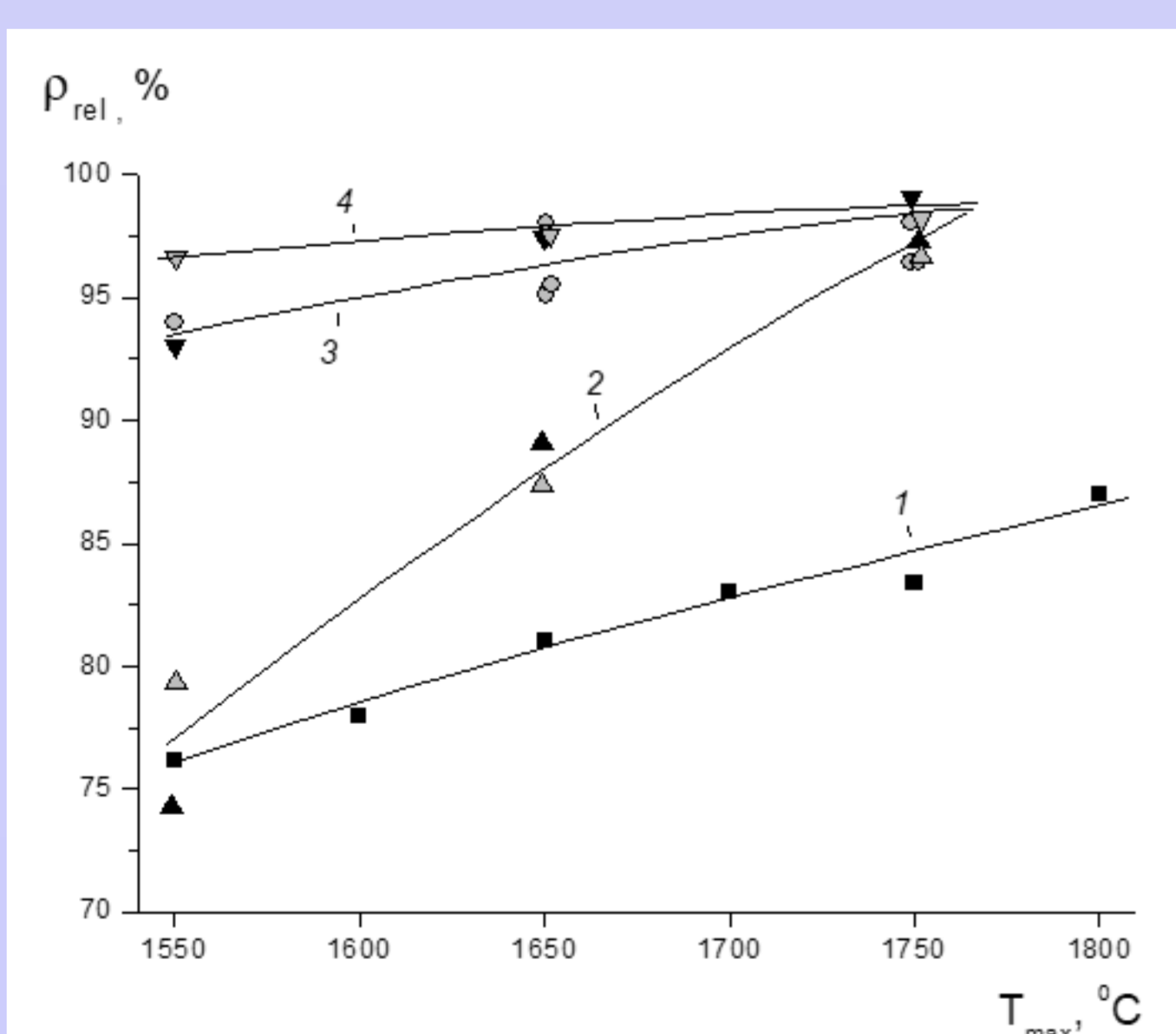


Figure 3. Relative density ρ_{rel} as a function of T_{max} for: (■) β -Si₂AlON₇ - curve 1, (○) β -Si₂AlON₇-BN (10–30 wt %) - curve 3, (▼) β -Si₂AlON₇-TiN (20 wt %)-BN (10 wt %) - curve 3, (□) β -Si₂AlON₇-TiN (40 wt %)-BN (10 wt %) - curve 4, (▲) β -Si₂AlON₇-SiC (20 wt %)-BN (10 wt %) - curve 2, (△) β -Si₂AlON₇-SiC (40 wt %)-BN (10 wt %) - curve 2.

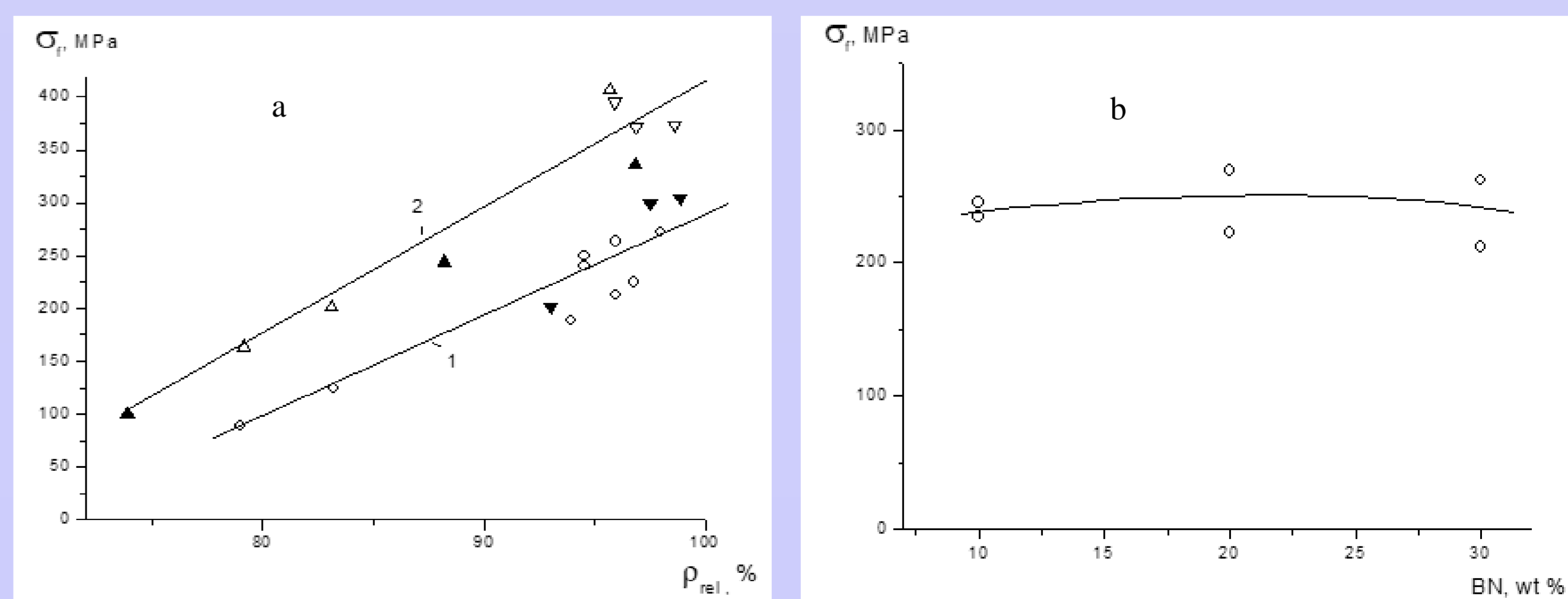


Figure 7. Flexural strength σ_f as a function of: (a) relative density ρ_{rel} for (○) β -Si₂AlON₇-BN (0–30 wt %) - curve 1, (▼) β -Si₂AlON₇-TiN (20 wt %)-BN (10 wt %), (▽) β -Si₂AlON₇-TiN (40 wt %)-BN (10 wt %) - curve 2, (▲) β -Si₂AlON₇-SiC (20 wt %)-BN (10 wt %), (△) β -Si₂AlON₇-SiC (40 wt %)-BN (10 wt %) - curve 2, and (b) BN content in β -Si₂AlON₇-BN (10–30 wt %) ($\rho_{rel} = 95-98\%$).

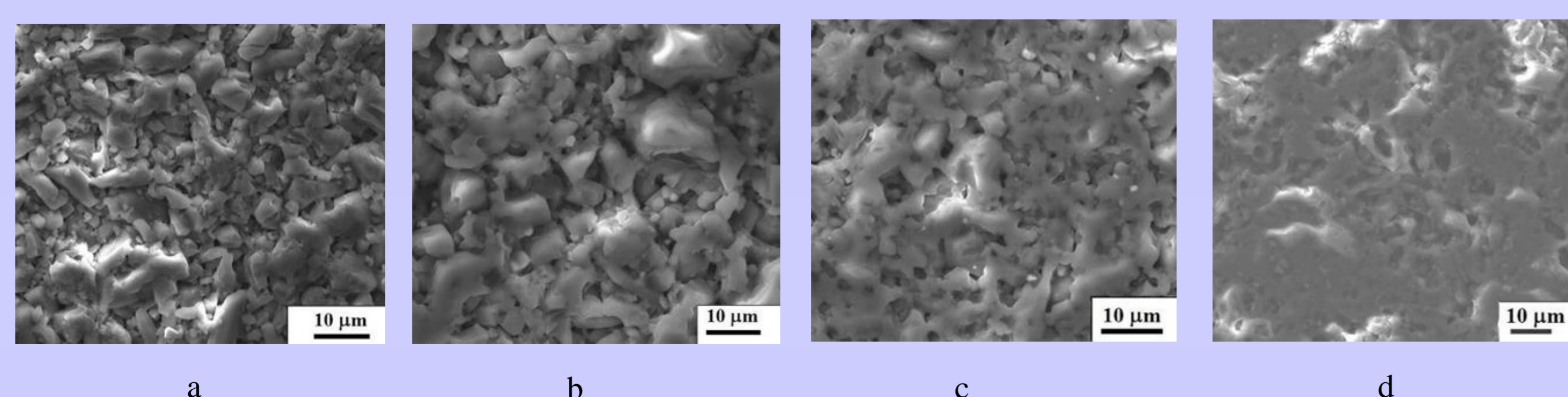


Figure 4. Fracture surface of β -Si₂AlON₇ sintered at 1550 (a), 1600 (b), 1700 (c), and 1800°C (d).

Conclusion

High-density β -SiAlON-based ceramic composites can be prepared by fast and energy efficient techniques: CS of raw powder materials and subsequent SPS. Thus obtained ceramics seem promising for fabrication of items for operating in conditions of strong thermal shock and in corrosive media.

Related references:

- Ekström, T. and Nygren, M., J. Am. Ceram. Soc., 75 (1992) 259–276.
- Liu G., Chen K.X., and Li J.T., Mater. Manu. Proc., 28 (2013) 113–125.
- Munir Z.A., Anselmi-Tamburini U., and Ohyanagi M., J. Mater. Sci., 41 (2006) 763–777.
- Kata D., Lis J., Pamphuch R., and Strobelski L., Int. J. Self-Propag. High-Temp. Synth., 7 (1998) 475–486.
- Zakorzhevskii V.V., Kovalev I.D., and Barinov Yu.N., Inorg. Mater., 53(2017) 278–286.
- Smirnov K.L., Int. J. Self-Propag. High-Temp. Synth., 24 (2015) 219–225.
- Zhang G.-J., Yang J.-F., Ando M., and Ohji T., Key Eng. Mater., 237 (2003) 123–128.